Ferroelectric-Monolayer Reconstruction of the $SrTiO_3$ (100) Surface

V. Ravikumar,[1] D. Wolf,[2] and V. P. Dravid[1]
[1]*Department of Materials Science and Engineering, Northwestern University, Evanston, Illinois 60201*
[2]*Materials Science Division, Argonne National Laboratory, Argonne, Illinois 60439*
(Received 11 October 1994)

Computer simulations of the two (100) surfaces of cubic $SrTiO_3$ show that the top layer of the SrO-terminated surface reconstructs to a ferroelectric-monolayer phase while the TiO_2-terminated surface remains bulklike. This behavior is shown to arise from a delicate crystal-environment sensitive competition between the long-range Coulomb and the short-range repulsive interactions.

PACS numbers: 68.35.Bs, 68.35.Md, 77.80.Dj, 77.84.Dy

With the rapidly advancing miniaturization of ferroelectric devices and the use of thin-film ferroelectrics and dielectrics in integrated electronic circuits, attention is gradually focusing on a possibly important role played by surfaces and interfaces in the overall performance of these materials and devices [1]. While it is well known that the bulk lattice phenomenon of ferroelectricity requires the existence of a strongly ionic, noncentrosymmetric crystal phase, the effect of the distinct crystallographic environments of surfaces and interfaces in bringing about—or possibly inhibiting—the formation of a ferroelectric phase is not nearly as well understood. Here we investigate the circumstances under which the free surface of a centrosymmetric crystal can become polar. By choosing a material for our simulations that does not form a ferroelectric *bulk* phase, any polarization phenomena may be attributed directly to the existence of the surface.

Most technologically important ferroelectric materials are oxides with a perovskite or a related structure which undergo a phase transition from the high-temperature cubic phase to a polar, noncentrosymmetric phase when cooled through the Curie temperature [2,3]. A notable exception is $SrTiO_3$, a prototype cubic perovskite, which remains cubic upon cooling [4,5]. The (100) surface of $SrTiO_3$ is used extensively as a substrate for epitaxial growth of high-T_c superconductors, particularly $YBa_2Cu_3O_7$ [6]. Also, the structure of perovskite surfaces is known to play a key role in surface reactions and catalysis [7]. $SrTiO_3$ is an interesting model system for computer simulations since we cannot only investigate the origin of bulk ferroelectricity in perovskites (by distorting the zero-temperature bulk cubic phase in the direction of the—unsuccessful—ferroelectric phase transition), but also elucidate the physical causes for the observed existence of a reconstructed, monolayer-thick polar phase in the SrO terminated, but not in the TiO_2-terminated, (100) surface (see Fig. 1), and compare with the reason for the absence of a bulk polar phase. Our main conclusion is that the behavior of both bulk $SrTiO_3$ and its two (100) surfaces is ruled by a delicate, *crystal-environment sensitive* balance between the long-range Coulomb interactions, which favor a polar phase, and the short-range (SR) repulsive interactions, which always favor a cubic environment.

The computational methods applied to determine the fully relaxed zero-temperature structure and energies of the free surfaces of $SrTiO_3$ involve iterative energy minimization combined with a fully ionic description of the interactions which include Coulomb and SR contributions. The SR interactions are described by a Buckingham-type empirical potential with values of the potential parameters given by Akhtar [8]. The parameters were derived by fitting to perfect crystal properties, and our calculations are only as representative of $SrTiO_3$ as the short-range parameters themselves. Ultimately the usefulness of this potential will be determined by how many properties of $SrTiO_3$ (other than those it was fitted to) it reproduces in agreement with the experiments. A region-I region-II strategy described elsewhere [9] was used to ensure that the surface region is properly attached to the bulk perfect crystal. Prior to considering the surfaces, we verified that the zero temperature perfect crystal does, indeed, choose the cubic perovskite structure.

For the case of cubic $SrTiO_3$, a fully ionic description is reasonably well justified, although for other perovskites, notably those exhibiting ferroelectric transitions at lower temperature (e.g., $BaTiO_3$) and particularly ones in which the alkaline earth ion is replaced by a transition-metal ion (e.g., $PbTiO_3$), such a description would be questionable

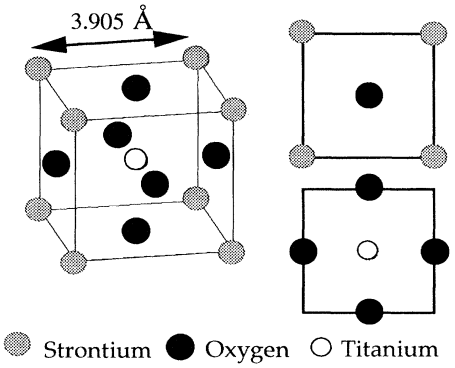

FIG. The cubic perovskite structure of $SrTiO_3$ (left) showing alternating SrO and TiO_2 planes along ⟨100⟩. The (100) surface can be either SrO or TiO_2 terminated (right).

 0031-9007/95/74(6)/960(4)$06.00

due to the importance of p-d hybridization associated with the delocalization of oxygen p states [3].

Initially, the primitive planar crystallographic unit cells of the two (100) surfaces shown in Fig. 1 were chosen as starting points for our simulations. While the unrelaxed energies of the two surfaces are the same (1735 mJ/m^2), upon relaxation the TiO_2-terminated surface assumes a slightly lower energy (of 1642 vs 1665 mJ/m^2, see Table I). As is common for ionic solids, both surfaces undergo "rumpling," with the larger anions moving out of and the smaller cations into the surface, and the two outermost interplanar spacings contract and expand, respectively.

To test the stability and uniqueness of the relaxed structures, several slightly disordered structures (in which the ions were randomly displayed from their bulk-terminated positions) were used as starting points for the relaxation while still maintaining the periodicity of the primitive planar unit cell. As a surprise, in addition to rumpling the SrO-terminated surface was found to reconstruct extensively by forming large static dipoles in the outermost plane of the surface (see Fig. 2), while the TiO_2 plane immediately underneath remained virtually unaffected. The related energy decreases to 1549 mJ/m^2 (see Table I). By contrast, the TiO_2-terminated surface maintains its fourfold rotation symmetry and does not reconstruct.

As shown in Fig. 2, the reconstruction results in a lateral displacement of rows of O^{2-} and Sr^{2+} ions in the outermost plane relative to each other, by –0.33 and +0.43 Å, respectively, giving rise to (a) a net surface-dipole moment and (b) a net translation of the top (SrO) plane with respect to the TiO_2 plane and the bulk crystal underneath. As is to be expected, since the unreconstructed surface has four-fold rotation symmetry, four equivalent reconstructions were obtained, depending on the directions of the initial displacements given to the ions in the unrelaxed surface.

One might ask whether the surface can reconstruct even further if the simulation cell is increased. This would, in principle, permit formation of a domainlike structure in which two or more of the four equivalent polar reconstructions coexist, involving 90° or 180° domain walls, or a combination of both. To test at least qualitatively whether domain formation is energetically favored, the size of the simulation cell was increased up to a 4 × 4 cell. The outcome is the "double-domain" surface structure shown in Fig. 3 in which two of the "microdomains" of Fig. 2 (with a size identical to the primitive planar unit cell) coexist in a regular, highly relaxed 2 × 2 pattern where adjacent "domains" are related by a ⟨110⟩ mirror plane. Again, as for the "single-domain" structure in Fig. 2, the reconstruction is limited to the surface layer. This (or one of the four cryptographically equivalent, ⟨110⟩-related) double-domain structure was obtained not only for a 2 × 2 simulation cell but also for 2 × 4, 4 × 2, and 4 × 4 simulation cells in which the ions were initially displaced randomly, and in a variety of ways. Although this does not prove that an even larger simulation cell would have given the same structure, it appears that this structure, with a remarkably low energy of 1143 mJ/m^2 (see Table I), is clearly very stable.

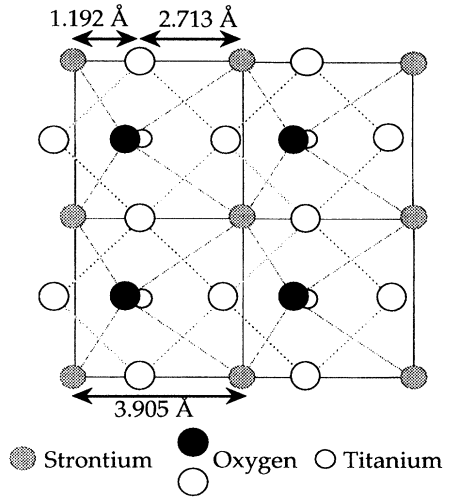

FIG. 2. One of the four cryptographically equivalent reconstructions of the SrO-terminated surface constrained to retain its bulk-terminated planar unit-cell periodicity; shown are four such unit cells.

TABLE I. Relaxed energies, $\gamma^{tot} = \gamma^C + \gamma^{SR}$, of the two (100) surfaces (in mJ/m^2). The energy differences $\Delta\gamma$ are taken relative to the values in the immediately preceding row. The unrelaxed energy of both bulk terminations is 1735 mJ/m^2.

	γ^{tot}	γ^C	γ^{SR}	$\Delta\gamma^{tot}$	$\Delta\gamma^C$	$\Delta\gamma^{SR}$
SrO-no recontruction	1665	3580	−1915	0	0	0
Single domain	1549	3055	−1506	−116	−525	409
Double domain	1143	3293	−2149	−406	238	−643
TiO_2-no reconstruction	1642	3876	−2234	0	0	0

Unfortunately, a comparison with previous studies provides little guidance as to how valid the above findings really are, although the (100) surface of $SrTiO_3$ has been the subject of many experimental [10–14] and two theoretical studies [4,15]. The latter give no indication for the existence of any reconstruction, although in agreement with our results for the unreconstructed surface, the results of Mackrodt [15] show a slight preference for the TiO_2 termination. In contrast to our simulations, low-energy [10] and reflection high-energy electron diffraction (LEED and RHEED) suggest that both (100) terminations coexist; however, photoelectron spectroscopy [12] and scanning tunneling microscopy (STM) [13,14] show a variety of surface structures, ranging from an ordered 2 × 2 superstructure of oxygen vacancies [14] to a series of reduced surface phases [13], which are thought to arise from different surface treatments and sublimation rates of Sr, Ti, and O that affect surface stoichiometry. In our simulations, by contrast, only the stoichiometric, defect-

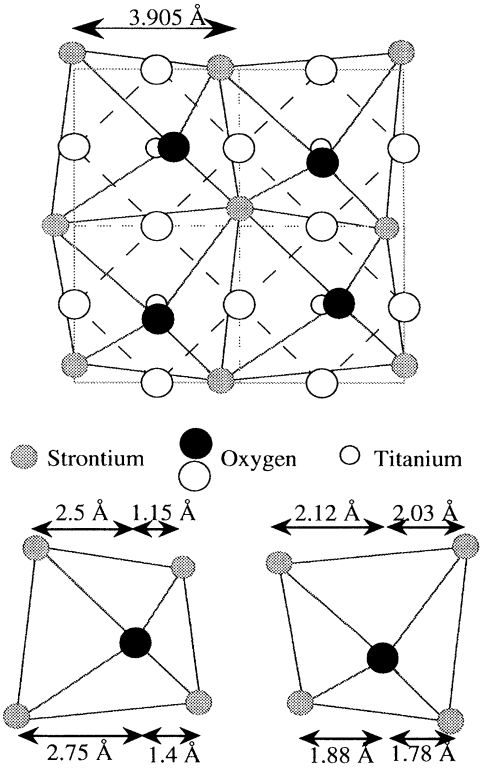

FIG. 3. Double-domain structure of the SrO-terminated surface obtained using a 2×2 simulation cell. The Sr^{2+} and O^{2-} rows are staggered, with average distances of 1.27 and 2.63 Å between them. The bulk unit cells are shown by dashed lines. The surface unit cells for the two domains are also shown.

free surfaces were considered. Hence the results cannot be compared with the STM studies which indicate nonstoichiometric or separate reduced surface phases. The LEED and RHEED results also depend on the surface treatments rendered [10,11]; also, the domains may not have been discerned due to various reasons like the inability to identify the exact termination of the surface, low fraction coverage of the surface and possible disorder in the microdomains, and very weak critical reflections from the reconstruction. However, recently McKee *et al.* [1] have reported layer-by-layer growth of $SrTiO_3$ and $BaTiO_3$ on MgO in which the perovskite structure was stabilized at the unit-cell level. The stabilization of such a surface should allow a test of the existence of 2D ferroelectricity and the transition to the well-known 3D structure and behavior of these materials.

We now consider the net electric polarization of the surfaces in Figs. 2 and 3. In the double-domain structure in Fig. 3, adjacent microdomains have orthogonal dipole moments, with net dipole moment of the surface along ⟨110⟩ [see Fig. 4(b) and Table II]. By contrast, in the single-domain surface Fig. 2 the dipole moment points along ⟨100⟩ [see Fig. 4(a)]. Although each microdomain in Fig. 4(b) exhibits a slightly larger net dipole

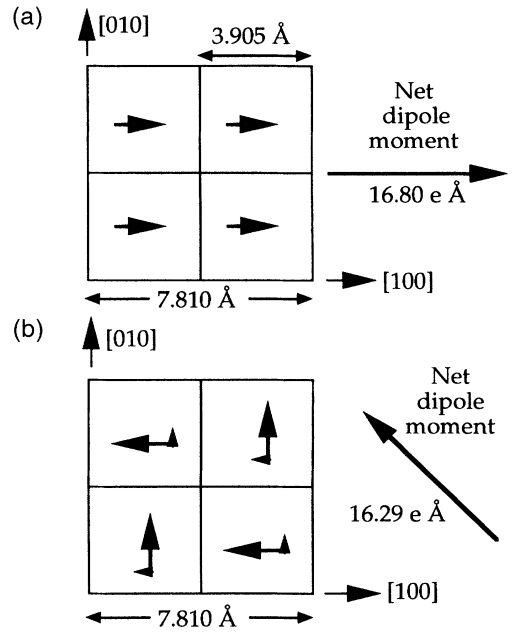

FIG. 4. Schematic representation of the dipoles in the surfaces in Figs. 2 and 3.

moment than the single-domain structure in Fig. 4(a), due to the 90° alignment of the domains, the surface polarization (i.e., the net dipole moment per unit area) is slightly smaller for the double-domain structure (see Table II). The formation of the domains in Fig. 4(b) thus leads to a reduction in the spontaneous surface polarization. Although we have not determined the absolutely lowest-energy domain configuration nor any effects of temperature (both of which require considerably larger simulation cells), the large energy decrease upon domain formation suggests a strongly attractive interaction between the domains, and therefore an indeed rather small domain size. We also note that by comparison, for example, with the dipole moment of 0.77 eÅ in the bulk unit cell of tetragonal $BaTiO_3$, the in-plane components of the surface moments in Table II are very large.

Starting from the structure in Fig. 3, one can anticipate that application of an electric field will lead to spontaneous polarization reversal by switching the surface

TABLE II. Components of the dipole moment **D** parallel (x, y) and perpendicular ($z \parallel [001]$) to the surface for various (see also Table I and Fig. 4) fully relaxed SrO-terminated surface structures (in units of e/Å, where e is the elementary charge). **P** is the net polarization of the surface layer ($|\mathbf{P}| = |\mathbf{D}|$/area, in units of e/Å).

	$\mathbf{D}_x$	$\mathbf{D}_y$	$\mathbf{D}_z$	$\lvert\mathbf{D}\rvert$	$\lvert\mathbf{P}\rvert$
No recontruction	0	0	0.64	0.64	0.042
Single domain	4.20	0	0.20	4.20	0.276
Double domain (each)	−5.40	0.36	0.16	5.41	0.355
Double domain (net)	−2.88	2.88	0.16	4.08	0.267

dipoles to variant directions. However, since we have not explicitly demonstrated the switchability of the polarization under an electric field, we cannot conclusively state that the polar monolayer phase is, indeed, ferroelectric. Nevertheless, the existence of long-range ordered static-displacement dipoles, the possibility of four energetically degenerate domain structures, and the coexistence of domains are remarkably similar in nature to the bulk ferroelectric phases of perovskites like $BaTiO_3$ and $PbTiO_3$. One might therefore wonder whether the underlying driving forces that cause—or prevent—formation of a polar phase are similar in the bulk and on the surface.

It has previously been suggested [3] that *bulk* ferroelectricity originates from a competition between the long-range Coulomb forces, which favor a polar phase, and the SR repulsive forces, which favor the nonpolar, cubic phase. To test this concept for the SrO-terminated surface, the total surface energy was broken down into its Coulomb and SR contributions (see Table I). Starting from the fully relaxed—but unreconstructed—surface, formation of static dipoles by the single-domain reconstruction is, indeed, driven by the Coulomb energy (which decreases by 525 mJ/m^2, thus more than compensating for the 409 mJ/m^2 increase in SR energy, see Table I line 2). Interestingly, however, subsequent formation of the double-domain structure is dominated by the SR repulsions which decrease (by 643 mJ/m^2) while the Coulomb energy actually increases (by 238 mJ/m^2, see Table I line 3). On balance, however, the net decrease in Coulomb energy relative to the unreconstructed surface (by 287 mJ/m^2) is still greater than the net decrease in SR energy (by 234 mJ/m^2). This analysis suggests distinct roles played by the Coulomb and SR forces: While the overall formation of the polar surface phase is driven Coulombicly, the domain formation (i.e., the attraction between the different domains) is driven by the SR repulsions, i.e., by ion size effects which give rise to the large lattice distortions shown in Fig. 3.

To further investigate the competition between Coulomb and SR forces in the formation of a polar phase, in particular its extreme sensitivity to the crystal environment, ions in both the SrO- and TiO_2-terminated surfaces and in bulk $SrTiO_3$ were given small displacements in the direction of the corresponding polar phase and the change in energy was monitored. It was found that in both types of crystal environments (surface vs bulk), the Coulomb forces favor the displacement while the SR forces always oppose it. Interestingly, Fig. 5 shows that when the Sr^{2+} ions in the SrO-terminated surface are displaced, the total energy reduces because the decrease in Coulomb energy is larger than the increase in Sr energy (see also Table I). By contrast, for identical Sr^{2+} displacements in a perfect-crystal environment, the decrease in Coulomb energy is more than compensated for by an increase in SR energy (see Fig. 5), pushing the ion back into the cubic site. This comparison demonstrates how sensitive the balance between the Coulomb and SR energies can be to the particular crystal environment. Similar displacements of Ti^{4+} in either the TiO_2-terminated surface or in the perfect crystal lead to the ion being pushed back into the cubic site due to the domination of the SR interactions—even though the Coulomb forces prefer the distortion.

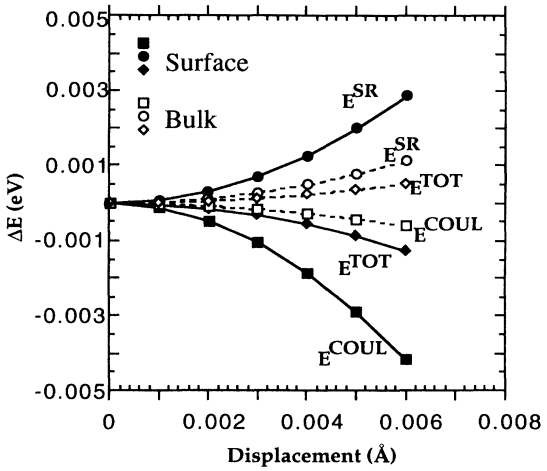

FIG. 5. Change in the Coulomb and SR contributions to the total energy for displacements of the Sr^{2+} ions (a) in the surface, from the bulk-terminated sites towards the polar structure in Fig. 2 and (b) in the bulk, from the cubic sites in the same direction.

This work was supported by the U.S. Department of Energy and BES Materials Sciences, the work of V.R. and V.P.D. under Grant No. DE-FG02-92ER45475, and that of D.W. under Contract No. W-31-109-Eng-38.

[1] R. A. McKee *et al.*, Phys. Rev. Lett. **72**, 2741 (1994).
[2] M. E. Lines and A. M. Glass, *Principles and Applications of Ferroelectrics* (Clarendon, Oxford, 1977).
[3] R. Cohen, Nature (London) **358**, 136 (1992); R. E. Cohen and H. Krakauer, Ferroelectrics **136**, 65 (1992).
[4] J. Prade *et al.*, J. Phys. Condens. Matt. **5**, 1 (1993).
[5] R. Cowley, Phys. Rev. **134**, A981 (1964).
[6] P. Chaudhari *et al.*, Phys. Rev. Lett. **58**, 2687 (1987).
[7] B. Cord and R. Courths, Surf. Sci. **162**, 34 (1985).
[8] M. J. Akhtar, Ph.D. thesis, University of Keele, 1990 (unpublished).
[9] D. Wolf, J. Am. Ceram. Soc. **67**, 1 (1984).
[10] N. Bickel *et al.*, Vacuum **41**, 46 (1990); Phys. Rev. Lett. **62**, 2009 (1989).
[11] T. Hikita *et al.*, J. Vac. Sci. Technol. A **11**, 2649 (1993).
[12] V. E. Henrich, G. Dresselhaus, and H. J. Zeiger, Phys. Rev. B **17**, 4908 (1978).
[13] Y. Liang and D. Bonnel, Surf. Sci. Lett. **285**, L510 (1993).
[14] T. Matsumoto *et al.*, Surf. Sci. Lett. **278**, L153 (1992).
[15] M. C. Mackrodt, Phys. Chem. Minerals **15**, 228 (1988).